Mat Stick–Derived CQD/Fe^{3+} Sensor for Ascorbic Acid Detection and Fluorescent Ink Applications

Manjushree Bera[a], Manik Das,[a, b] Arjina Khatun[b], Subrata Mukhopadhyay[b], Bidhan Chandra Samanta[c], Tithi Maity[a]*

[a] Department of Chemistry, Natural Science Research Center, Prabhat Kumar College (Vidyasagar University) Contai, Purba Medinipur, India, 721404

[b]Department of Chemistry, Jadavpur University, Jadavpur, Kolkata, West Bengal, India

[c] Department of Chemistry, Mugberia Gangadhar Mahavidyalaya, Purba Medinipur, India

Email: titlipkc2008@gmail.com

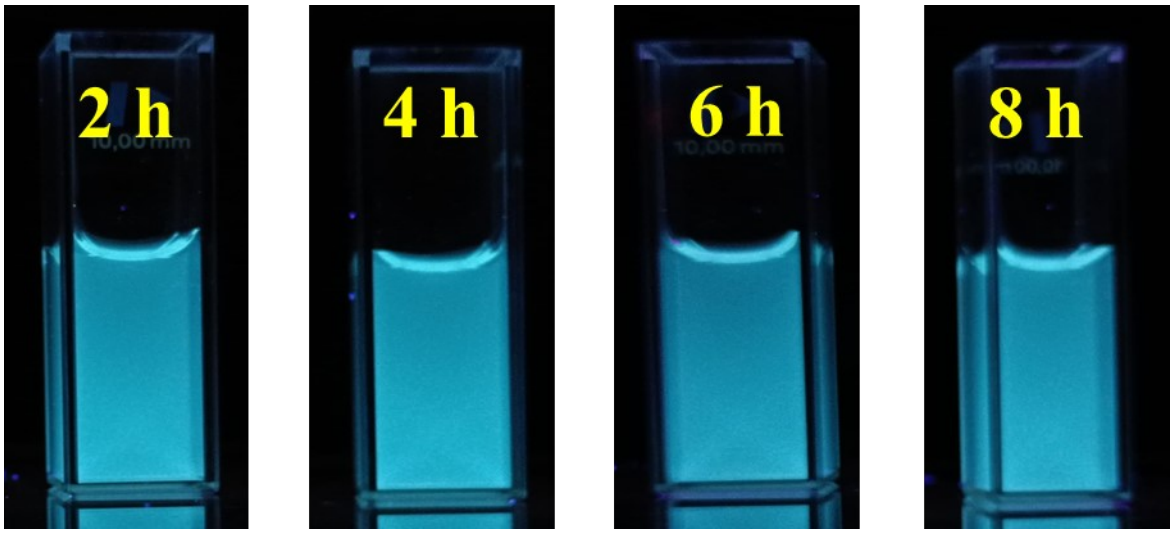

Figure S1: Observation of the fluorescence colour of the synthesized CQDs as a function of time under the UV light (λ_{max} = 365 nm) to investigate the photo stability of the CQDs.

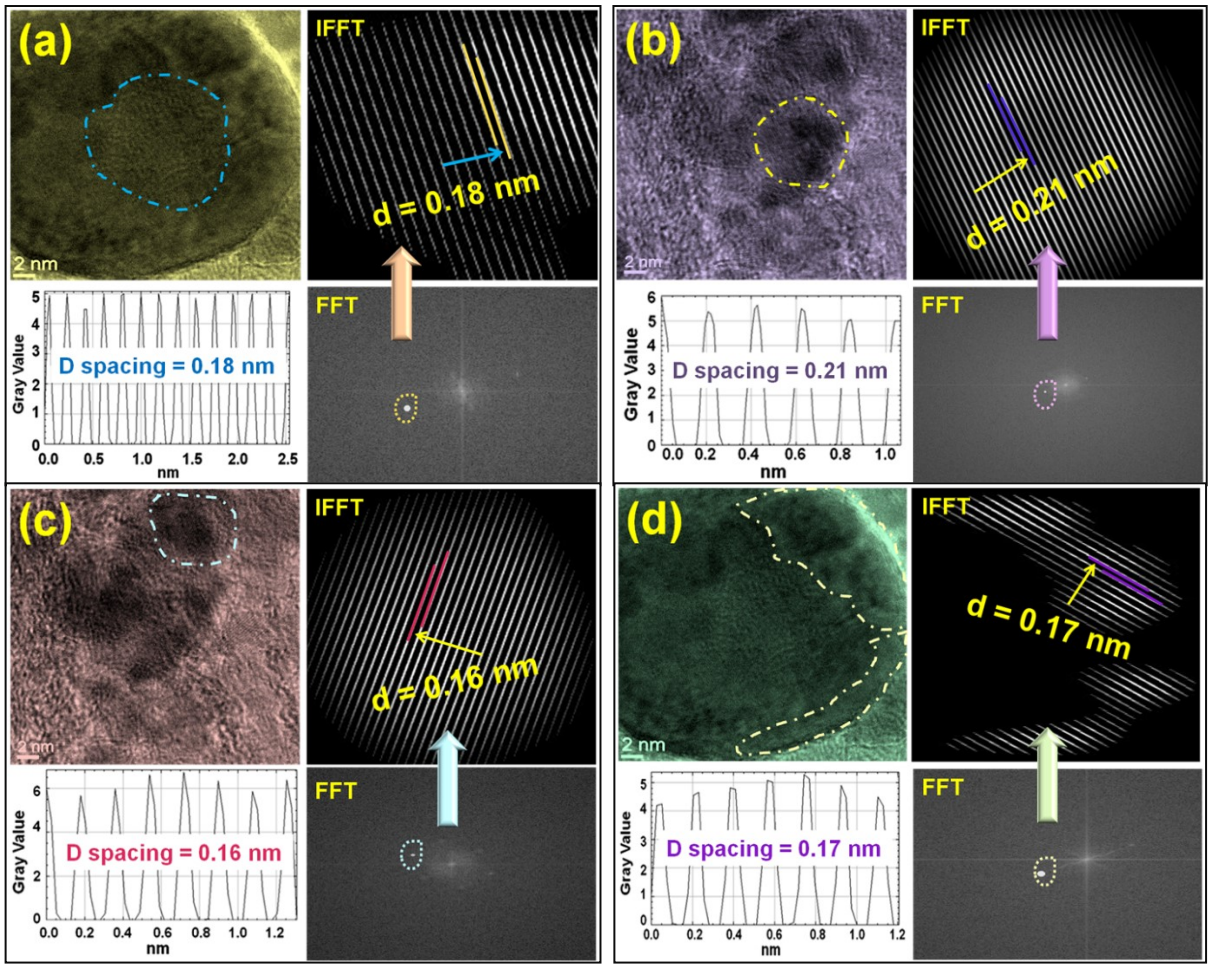

Figure S2. (a-d) FFT and IFFT images of CQDs with their respective surface profile.

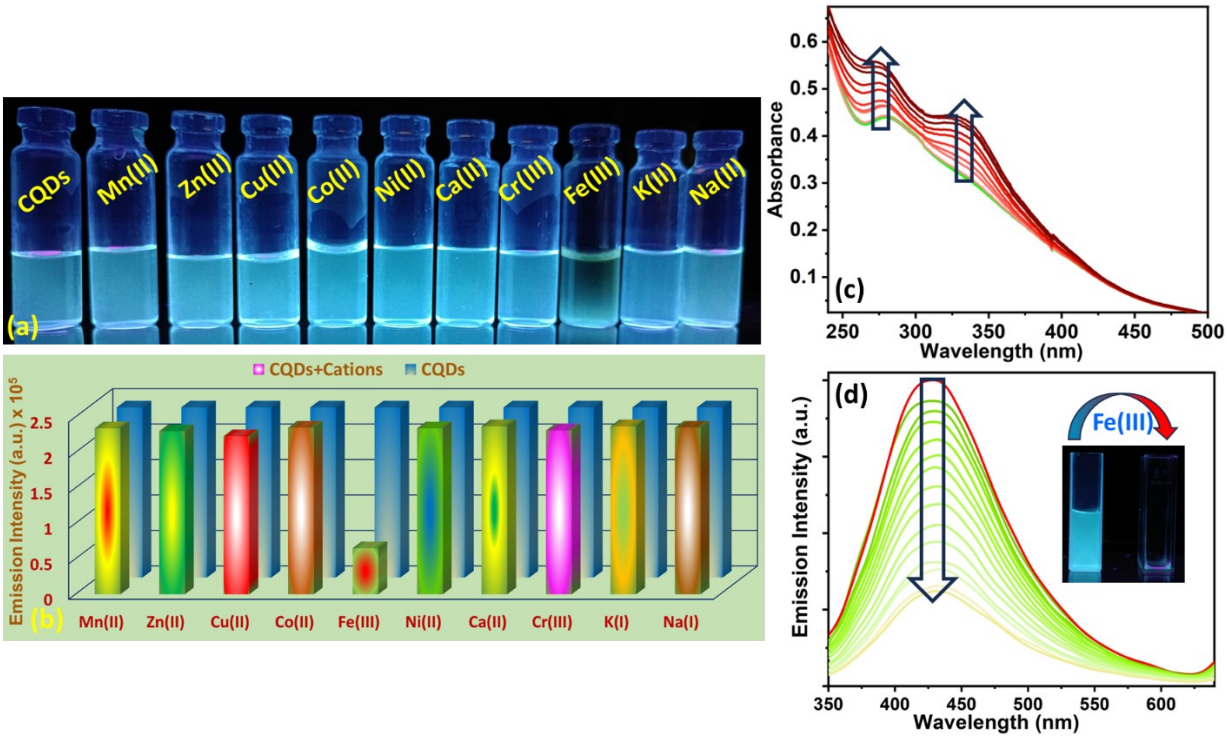

Figure S3: (a) Optical colour change of CQDs upon addition of several cations under the UV light (λ_{max} = 365 nm) (b) Fluorescence intensity change of CQDs at λ_{em} = 430 nm after the addition of several cations upon excitation λ_{ex} = 330 nm, (c) UV-vis spectral titration graph of CQDs after the gradual addition of Fe(III) (1- 15 μM) (d) Fluometric spectral titration graph of CQDs after the gradual addition of Fe(III) (1- 20 μM)

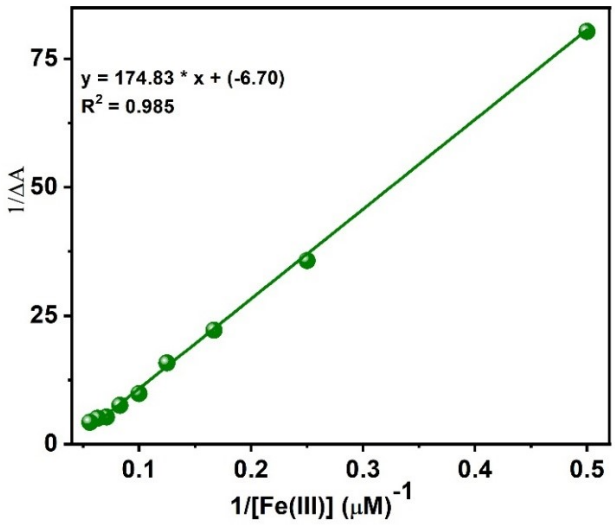

Figure S4: Binding constant determination plot of CQDs/Fe complex.

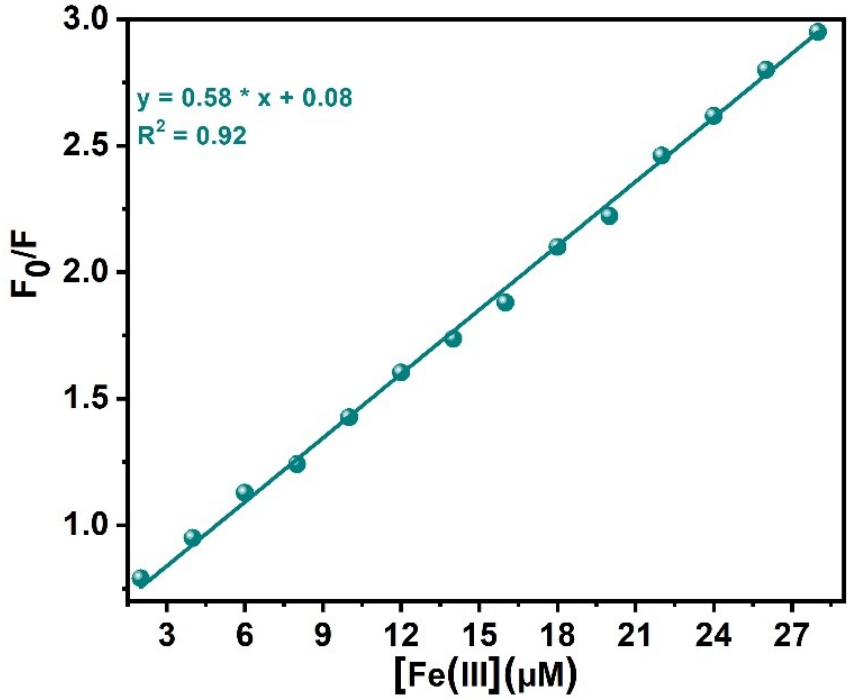

Figure S5: The Stern-Volmer quenching constant plot of CQDs-Fe(III) adduct.

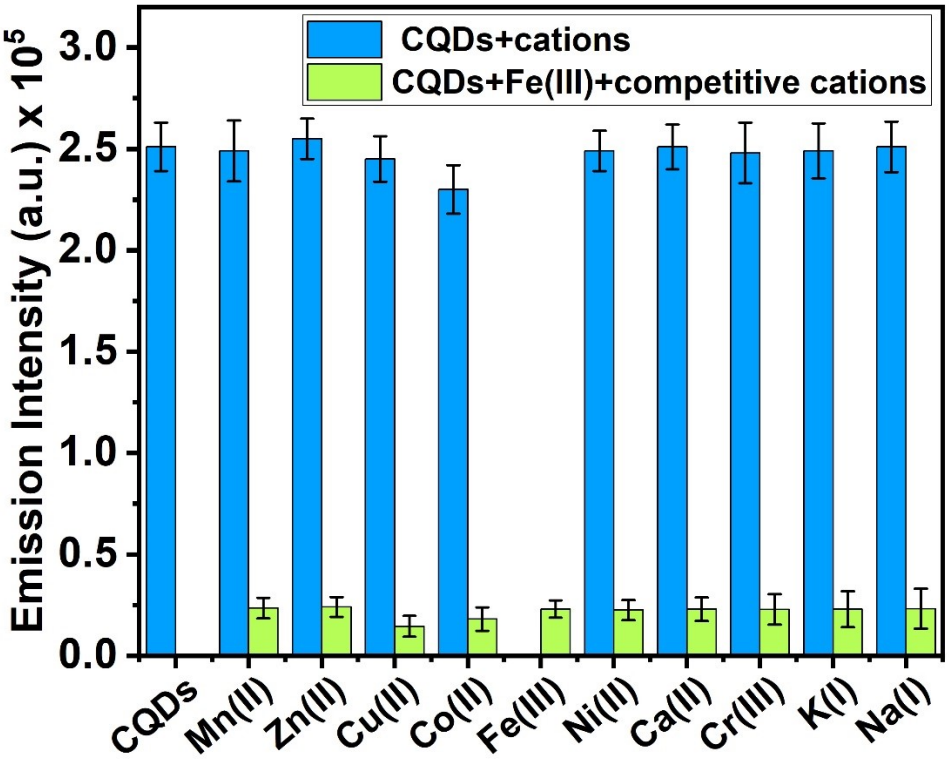

Figure S6: Competitive cation interference plot of CQDs for Fe(III) detection

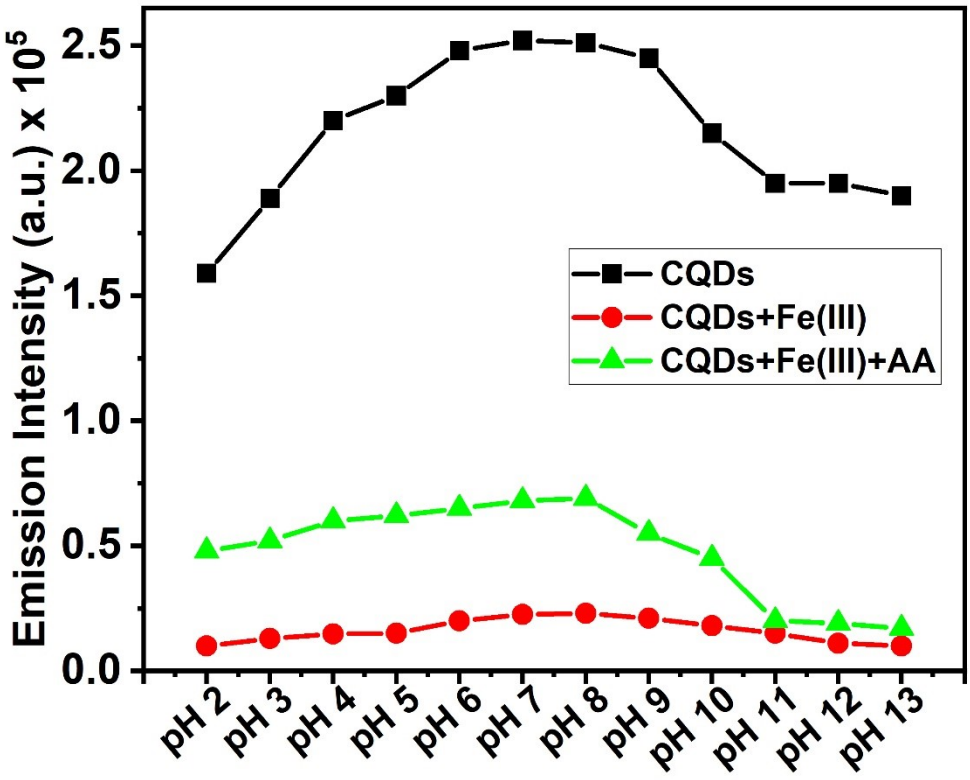

Figure S7: Effect of pH on the fluorescence intensity of the synthesized CQDs and its daughter complexes

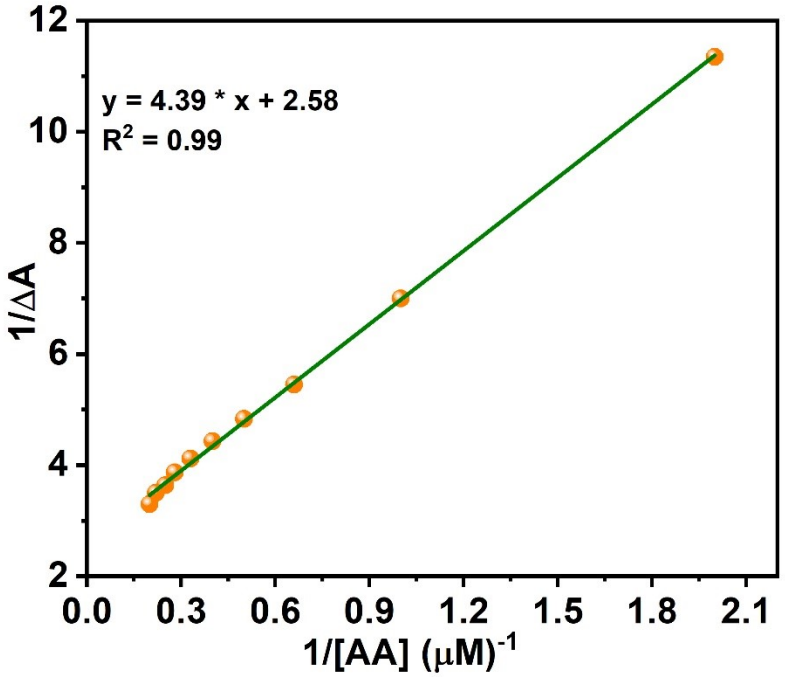

Figure S8: The B-H equation plot for the binding constant determination of CQDs/Fe complex with ascorbic acid at 270 nm.

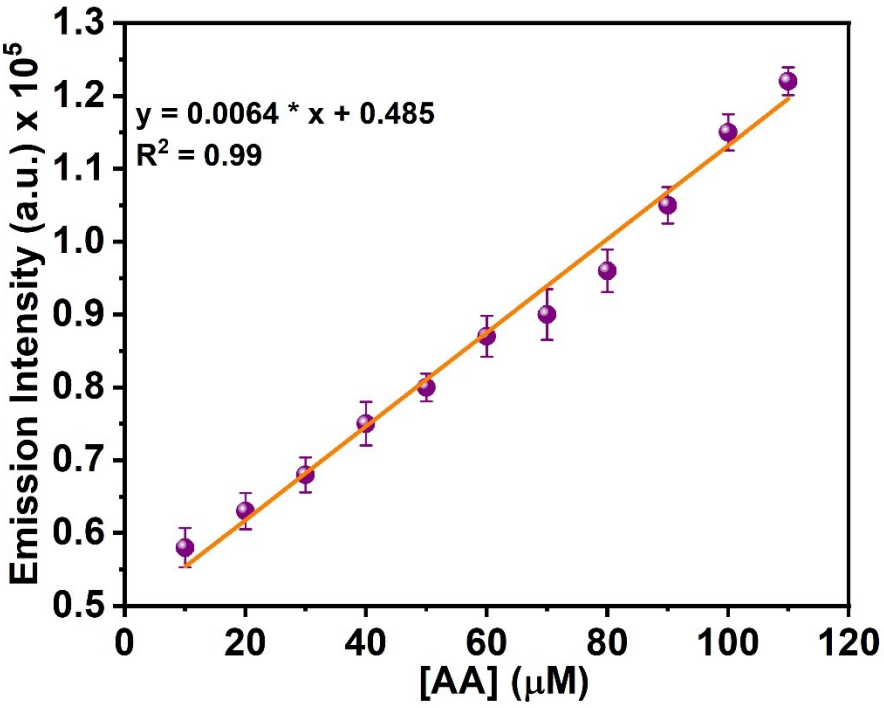

Figure S9: Change of emission intensity of CQDs/Fe vs concentration of AA plot for the determination of LOD value.

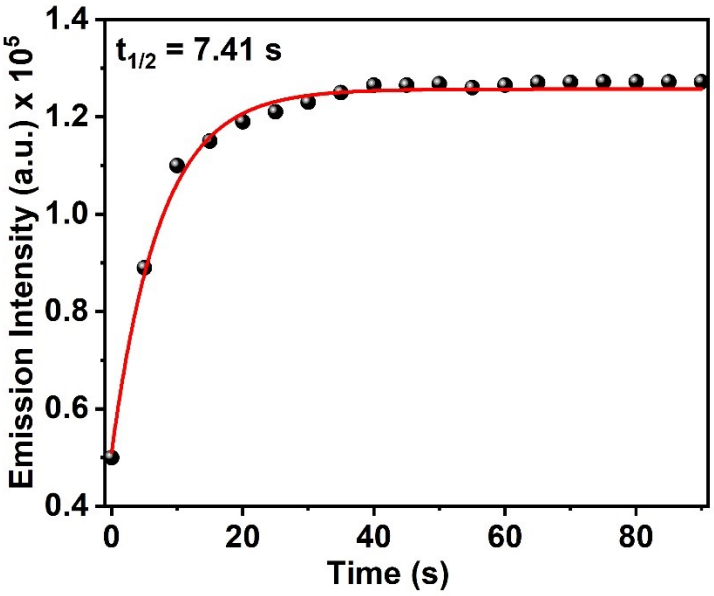

Figure S10: Time response emission intensity enhancement graph curve for CQDs/Fe(III) during the detection of AA.

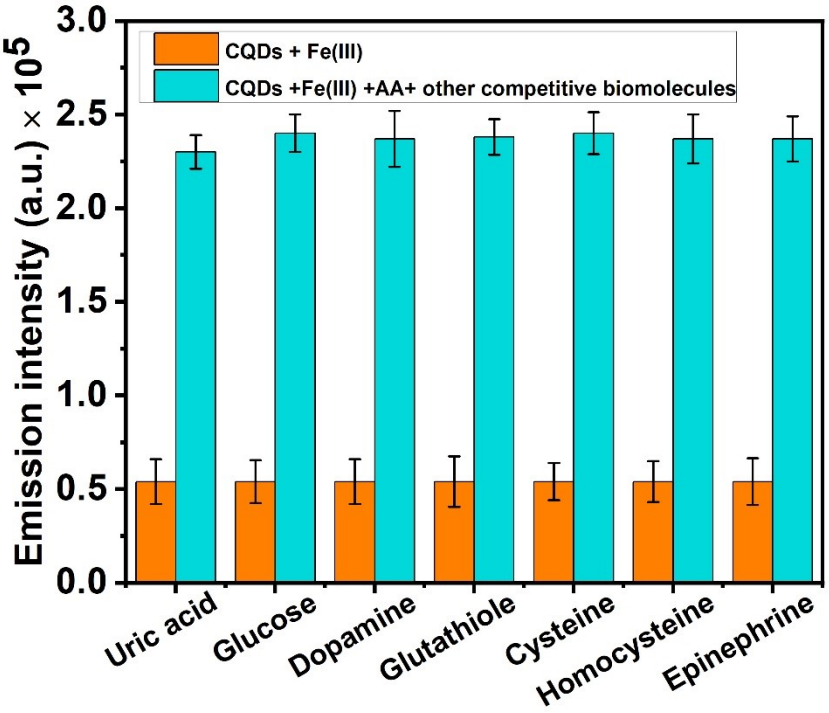

Figure S11: Competitive biomolecules interference plot of CQDs/Fe complex for the detection of ascorbic acid.

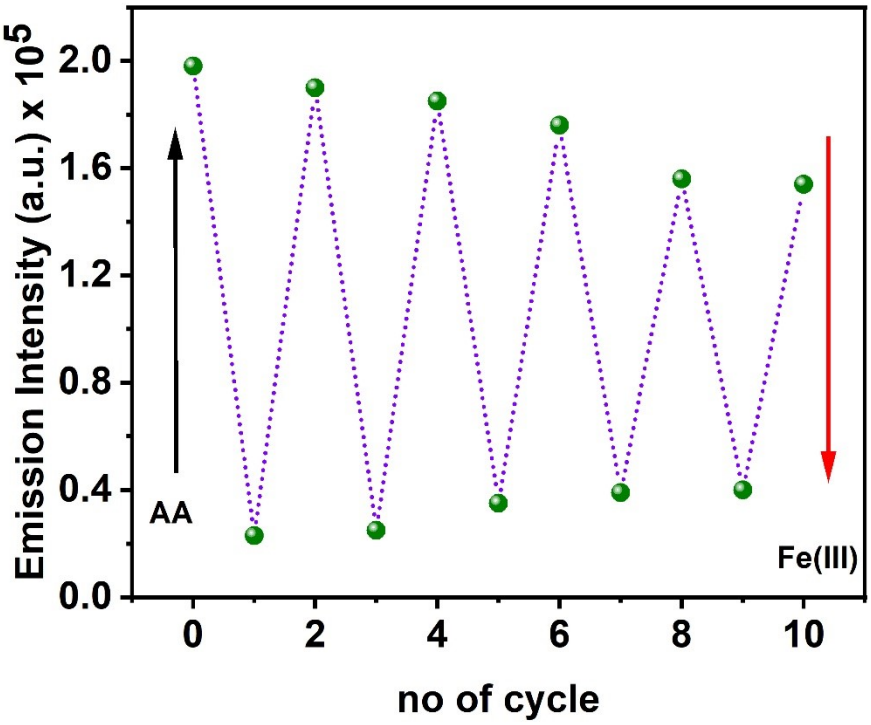

Figure S12: Reproducibility confirmation of CQDs/Fe(III) complex during detection of AA, which is monitored by the alternative addition of AA and Fe(III) in the CQDs/Fe solution.

Figure S13: Detection of AA by CQDs/Fe(III) as paper strip (Left side only QCDs, middle QCDs +Fe(III) and right side QCDs +Fe(III)

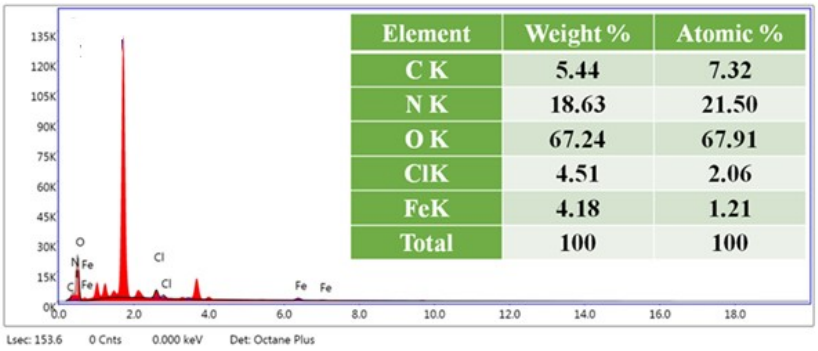

Element	Weight %	Atomic %
C K	5.44	7.32
N K	18.63	21.50
O K	67.24	67.91
ClK	4.51	2.06
FeK	4.18	1.21
Total	100	100

Figure S14: EDAX spectra of CQDs/Fe complex with their respective elements. [Inset: table of percentages of elements]

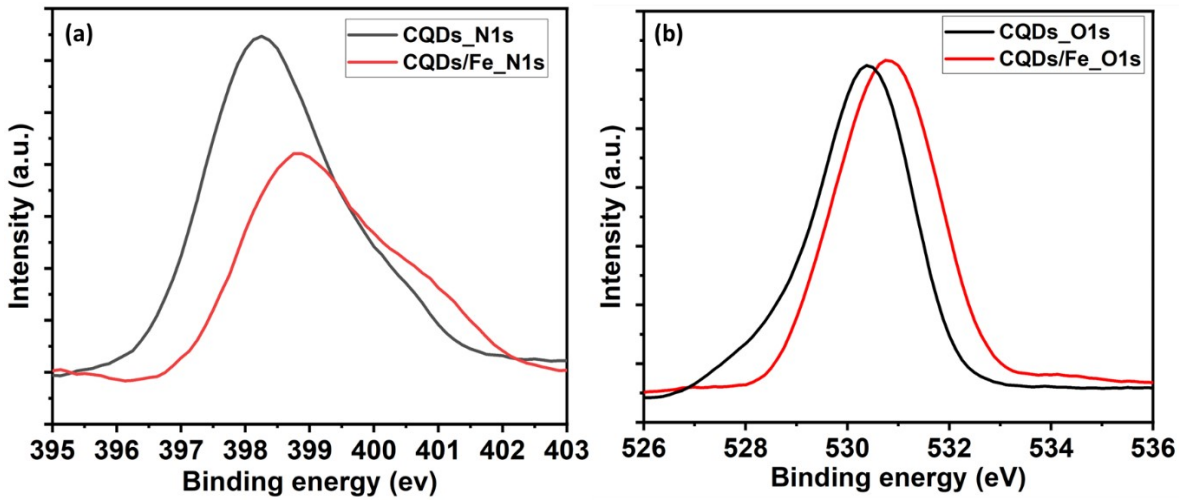

Figure S15: XPS graph (a) N1s and (b) O1s showing the of binding energy shifting of the donor atoms after coordination with the metal ion.

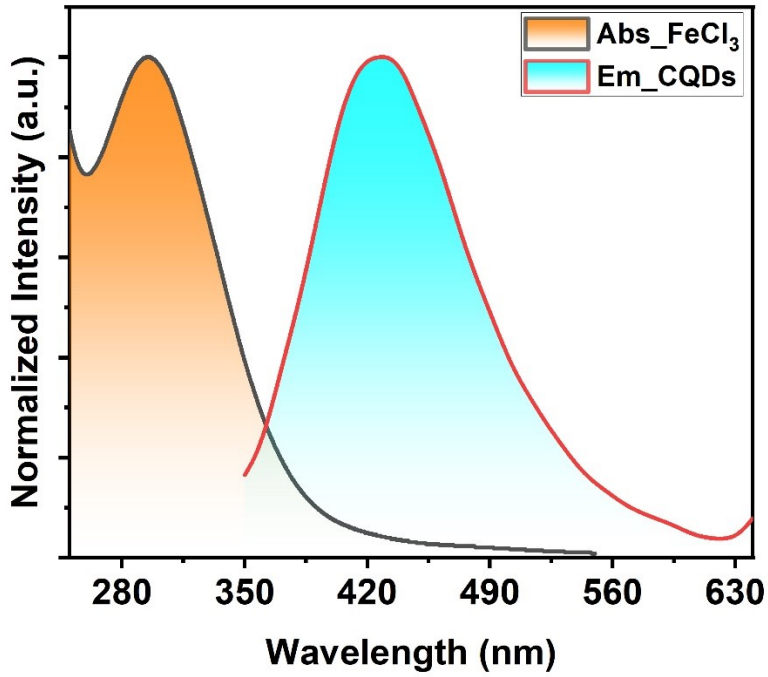

Figure S16: Spectral overlap between $FeCl_3$ absorption and CQDs emission.

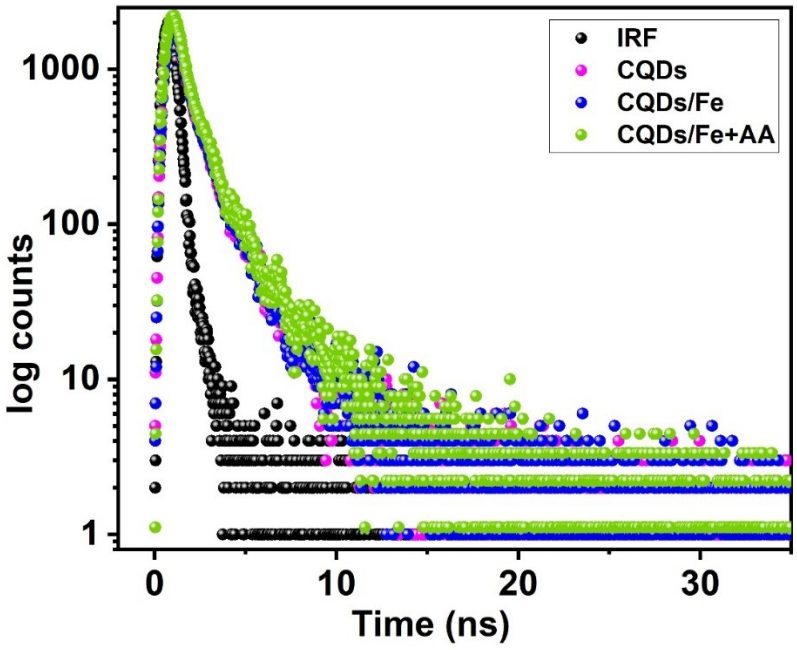

Figure S17: The fluorescence lifetime graph of the CQDs before and after the addition of Fe(III) and Ascorbic acid (AA).

Table S1: Fluorescence lifetime decay table

sample	α_1	α_2	τ_1	τ_2	τ_{av}	χ_2
CQDs	0.76	0.24	2.99	1.65	2.66	1.02
CQDs/Fe	0.83	0.17	2.57	1.42	2.37	1.24
CQDS/Fe+AA	0.82	0.18	2.86	1.45	2.60	1.18

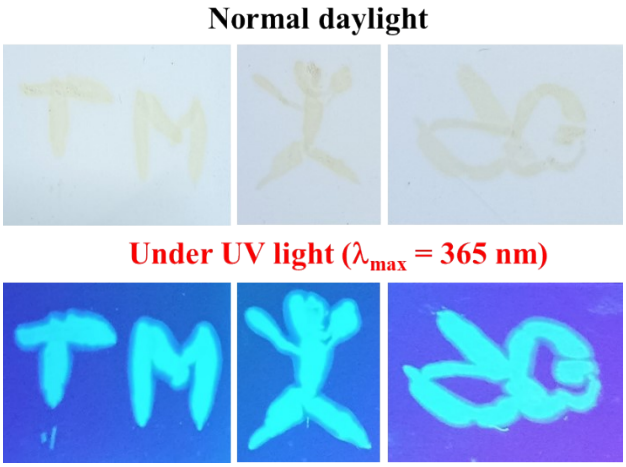

Figure S18: Calligraphy works drawing using the CQDs solution as fluorescent ink.